HKU CS Tech Report TR-2005-03

# Continuous Collision Detection for Elliptic Disks

Yi-King Choi, Wenping Wang, Yang Liu *
Department of Computer Science, The University of Hong Kong, Hong Kong

Myung-Soo Kim
Department of Computer Eng., Seoul National University, Seoul, South Korea

**Abstract**

Collision detection and avoidance is important for various tasks in robotics. Compared with commonly used circular disks, elliptic disks provide compact shape representation for robots or other vehicles confined to move in the 2D plane. Furthermore, elliptic disks allow simpler analytic representation than rectangular boxes do; this makes it easier to perform continuous collision detection. We shall present a fast and accurate method for continuous collision detection between two moving elliptic disks; *continuous collision detection* does not need to sample the time domain of motion, thus avoiding missing possible collision between time samples. Based on some new algebraic conditions on the separation of two ellipses, we reduce collision detection for two moving ellipses to the problem of detecting real roots of a univariate equation which is the discriminant of the characteristic polynomial of the two ellipses. Various techniques are investigated in detail for robust and accurate processing of this univariate equation for two classes of commonly used motions: (1) planar screw motions; and (2) planar rational motions, i.e. motions that can be represented as rational functions of the time parameter $t$. Experimental results are presented to demonstrate the efficiency, accuracy and robustness of our method.

*Keywords* — ellipses, elliptic disks, rational motion, collision detection, interference analysis

## 1 Introduction

Collision detection is important in robotics for path planning or simulation. Avoidance of collision between moving objects is greatly facilitated by accurate collision detection

*This work was supported by the Research Grant Council of Hong Kong.

algorithms. In applications where real-time response is mandatory, the efficiency of collision detection algorithms is also of high importance. Although many collision detection algorithms are catered for 3D applications [12], there are still numerous other applications in which moving objects are confined to be in the 2D plane. Some examples are from robot or vehicle path planning where the robots and vehicles represented by 2D figures move in the 2D plane, and the robot movements may follow any paths with arbitrary rotations. When there are more than one robot moving in the same space, collision detection between these robots becomes critical. Apart from equipping the robots with sensors for online collision avoidance, it is often also necessary to have the robot paths planned and verified in advance.

Even in the 2D setting, the outline of an object can be quite complex. In this case a two-phase approach to collision detection is widely adopted in practice. To facilitate the collision detection process, objects are often enclosed by simple geometric entities, which we shall call *enclosing objects* (also called *bounding objects* in the literature), so that simpler collision detection can first be performed on these enclosing objects; more complicated computation on collision detection for the original objects will only be carried out after their enclosing objects have been detected to be overlapping.

The commonly used enclosing objects include circular disks and rectangles. There are, in general, two criteria in choosing the type of enclosing objects to be used in a particular application. The first is about *bounding tightness*; that is, enclosing objects should be as tight as possible so that when two enclosed objects are separate, their enclosing objects should be separate most of the time. This criterion serves to save time by ensuring that many non-colliding pairs are not subject to further processing once their enclosing objects are found to be separate. The second criterion is that the collision detection for a pair of enclosing objects should be simple and very fast, since this operation normally needs to be done many times, i.e. for every pair of objects present in an environment. Thus, based on these considerations, it is not hard to understand why circular discs (and spheres in 3D case for this matter) are commonly used as bounding objects of robots in the plane (e.g. [17]); collision detection for a pair of circles is almost trivial, therefore can be performed very efficiently. Interference testing of circular discs has also well been studied in computational geometry [18, 23, 24].

Ellipses provide a much tighter bounding volume than circles. When a union of ellipses or circles are used, normally far fewer ellipses are needed than circles to enclose a given object with the same degree of tightness. Therefore the use of ellipses as enclosing objects can potentially lead to significant improvement of accuracy and efficiency in collision detection. However, little work can be found in the literature on using ellipses as enclosing objects, largely because of the lack of effective means of detecting collision for ellipses. Overall, there are several major issues in using ellipses as enclosing objects; these include computing the smallest enclosing ellipse of a given object, detecting collision of two moving ellipses, and computing the penetration distance of two overlapping ellipses, etc. In this paper we shall focus on collision detection of two elliptic disks with pre-specified continuous motion. (We shall sometimes use the terms *ellipse* and *elliptic disk* interchangeably, when there is no danger of confusion. Strictly speaking, an elliptic disk comprises the boundary

points and interior points of an ellipse.)

Thorough analysis and classification of intersection of general conics can be found in classical algebraic geometry, e.g. [1, 2]. These results are, however, for conics in the complex (projective, affine or Euclidean) plane, and are therefore not applicable to our application under consideration, where the analysis must be done in the real plane. A straightforward but brute-force approach to detecting intersection between stationary ellipses is to compute their real intersection points. This entails the numerical solution of a quartic equation and is thus difficult to be extended to deal with two moving ellipses.

A typical approach to collision detection of moving objects over a time interval is to sample the time interval at discrete instants and test whether two objects intersect at each sampled time instant. This temporal sampling approach is prone to error, since it may miss collisions that occur in-between sample instants, although it is possible to reduce such error by raising the sampling resolution at the expense of increased computation for overlap testing. There have been attempts to use the speed bound of moving objects to determine a safe time sampling resolution [4].

We shall present a fast and accurate algorithm for collision detection between two moving ellipses in the 2D plane. We use some new conditions on the separation of two ellipses to reduce the collision detection problem of two moving ellipses to the problem of detecting a real zero of a univariate function which is the discriminant of the characteristic polynomial of the two ellipses. This algebraic approach makes our method fast and accurate, since we do not need to approximate the shape of ellipses or sample the time interval of motion.

Our method is based on theoretical results similar to those in [26] about the separation of two stationary ellipsoids in 3D space, but there are fundamental differences between these results for ellipses and ellipsoids. First, the separation condition for two stationary ellipses cannot be derived as a special case from the result in [26] on two stationary ellipsoids, although the former is a low-dimension counterpart of the latter. Therefore, in this paper we shall prove for the first time an algebraic condition on the separation of two stationary ellipses. Second, compared with ellipsoids, the characteristic polynomial of two ellipses has relative simple properties, and this simplicity allows us to reduce their collision detection in the moving case to a problem of detecting the zero of a univariate function. But such a treatment is, in general, not possible for two moving ellipsoids, at least not in the same straightforward manner, as will be discussed in detail later. Our approach addressing this issue for collision detection of moving ellipsoids is reported in [5], which is based on zero-set analysis of a bivariate function.

The contributions of this paper are the following:

1. A simple algebraic condition for the separation of two stationary ellipses is established;

2. An algebraic condition for detecting collision of two moving ellipses is established;

3. Based on the above conditions, we propose an algorithmic framework for fast and accurate collision detection of two moving ellipses. We discuss in detail two classes

of commonly used motions: the screw motions and rational motions. In particular, to achieve reliable collision detection, we present robust methods for processing high degree polynomials arising from the use of rational motions.

The remainder of this paper is organized as follows. In Section 2, we shall establish the algebraic condition for the separation of two stationary ellipses and other algebraic properties of the configuration formed by a pair of ellipses. Then these results are used in Section 3 to prove a separation condition for two moving ellipses. The framework of our collision detection algorithm is presented in Section 4. In Section 5 we discuss details on the formulation and processing of the screw motion, which is a simple but commonly used non-rational motion. In Section 6 we present algorithms for ellipses moving in rational motions, concentrating on devising numerically stable algorithms for processing high degree polynomials arising from rational motions. We conclude the paper and discuss further research problems in Section 7.

# 2 Condition on Separation of Two Ellipses

In this section, we are going to prove the separation condition of two stationary ellipses. An ellipse, as a conic section curve, in 2D Euclidean plane $\mathbb{E}^2$ is defined by $X^TAX = 0$, where $A = [a_{i,j}]$ is a $3 \times 3$ real symmetric matrix, and $X$ is a 3D column vector for the homogeneous coordinates of a point in $\mathbb{E}^2$. Let $A_{i,i}$ denote the leading submatrix of size $i \times i$ of $A$, $i = 1, 2, 3$. For an ellipse $X^TAX = 0$ we shall assume throughout that the matrix $A$ is normalized such that $\bar{X}^TA\bar{X} < 0$ for any interior point $\bar{X}$ of $\mathcal{A}$. Then by elementary geometry, an ellipse $X^TAX = 0$ is characterized by that $\det(A_{1,1}) = a_{1,1} > 0, \det(A_{2,2}) > 0$, and $\det(A_{3,3}) < 0$. Thus, $A_{2,2}$ is positive definite.

An *elliptic disk* $\mathcal{A}$ is defined by $\mathcal{A} \equiv \{X | X^TAX \leq 0\} \subset \mathbb{E}^2$. We use $\partial\mathcal{A}$ to denote the boundary curve of $\mathcal{A}$, i.e. the set of point satisfying $X^TAX = 0$, and use $\mathrm{Int}(\mathcal{A})$ to denote the interior points of $\mathcal{A}$. Thus, $\mathcal{A} = \partial\mathcal{A} \cup \mathrm{Int}(\mathcal{A})$. For brevity, we sometimes use the terms *ellipse* and *elliptic disk* interchangeably when there is no danger of confusion.

Two elliptic disks $\mathcal{A} : X^TAX \leq 0$ and $\mathcal{B} : X^TBX \leq 0$ are said to be *separate* or *disjoint* if $\mathcal{A} \bigcap \mathcal{B} = \emptyset$. The disks $\mathcal{A}$ and $\mathcal{B}$ are said to be *overlapping* if $\mathrm{Int}(\mathcal{A}) \bigcap \mathrm{Int}(\mathcal{B}) \neq \emptyset$. The disks $\mathcal{A}$ and $\mathcal{B}$ are said to be *touching* if $\mathcal{A} \bigcap \mathcal{B} \neq \emptyset$ and $\mathrm{Int}(\mathcal{A}) \bigcap \mathrm{Int}(\mathcal{B}) = \emptyset$ (see Fig. 1).

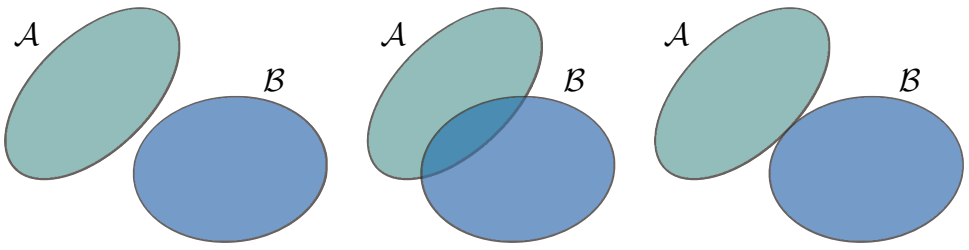


(a) $\mathcal{A} \cap \mathcal{B} = \emptyset$ (b) $\mathcal{A} \cap \mathcal{B} \neq \emptyset$ (c) $\mathcal{A} \cap \mathcal{B} \neq \emptyset$ and $\mathrm{Int}(\mathcal{A}) \cap \mathrm{Int}(\mathcal{B}) = \emptyset$

Figure 1: Two elliptic disks $\mathcal{A}$ and $\mathcal{B}$ are (a) separate; (b) overlapping; and (c) touching.

Given two elliptic disks $\mathcal{A} : X^T AX \leq 0$ and $\mathcal{B} : X^T BX \leq 0$, the cubic polynomial $\mathrm{f}(\lambda) = \det(\lambda A - B)$ is called the *characteristic polynomial* and $\mathrm{f}(\lambda) = 0$ the *characteristic equation* of $\mathcal{A}$ and $\mathcal{B}$.

**Lemma 1** *For any two elliptic disks $\mathcal{A} : X^T AX \leq 0$ and $\mathcal{B} : X^T BX \leq 0$, the root pattern of $\mathrm{f}(\lambda) = 0$ is in one of the following three cases:*

1. *three positive roots; or*
2. *one positive and two negative roots; or*
3. *one positive and a pair of complex conjugate roots.*

**Proof:** Suppose

$$\mathrm{f}(\lambda) = a_3\lambda^3 + a_2\lambda^2 + a_1\lambda + a_0.$$

Then $a_3 = \det(A) < 0$ and $a_0 = -\det(B) > 0$. It follows that $\mathrm{f}(0) > 0$ and $\mathrm{f}(+\infty) < 0$. Hence, $\mathrm{f}(\lambda) = 0$ has at least one positive root. Moreover, since $a_3 \neq 0$ and $a_0 \neq 0$, 0 or $\infty$ cannot be a root of $\mathrm{f}(\lambda) = 0$. Let $\lambda_0 > 0$, $\lambda_1$ and $\lambda_2$ denote the three roots. Since $\lambda_0\lambda_1\lambda_2 = -a_0/a_3 > 0$, we have $\lambda_1\lambda_2 > 0$. Hence, the other two roots $\lambda_1$ and $\lambda_2$ can only be either both positive, or both negative, or a pair of complex conjugates. □

**Lemma 2** *If $\mathrm{Int}(\mathcal{A}) \bigcap \mathrm{Int}(\mathcal{B}) = \emptyset$, then $\mathrm{f}(\lambda) = 0$ has a negative root.*

**Proof:** Since $\mathrm{Int}(\mathcal{A}) \bigcap \mathrm{Int}(\mathcal{B}) = \emptyset$, we may suppose that $\mathcal{A}$ and $\mathcal{B}$ are either separate or touching externally. By the substitution $\lambda = (\mu - 1)/\mu$, which maps $\mu \in [0, 1]$ to $\lambda \in (-\infty, 0]$, the characteristic equation $\mathrm{f}(\lambda) = \det(\lambda A - B) = 0$ is transformed to $\mathrm{g}(\mu) \equiv \det((1 - \mu)A + \mu B) = 0$. Denote $Q(\mu) \equiv (1 - \mu)A + \mu B$. Note that $Q(0) = A$ and $Q(1) = B$. Clearly, $\mathrm{f}(\lambda) = 0$ has a finite negative root if and only if $\mathrm{g}(\mu) = 0$ has a real root in $(0, 1)$. We shall show by contradiction that $\mathrm{g}(\mu) = 0$ has a real root in $(0, 1)$.

Assume that $\mathrm{g}(\mu) = 0$ has no real root in $(0, 1)$. Since $\mathrm{g}(\mu) \equiv \det((1 - \mu)A + \mu B)$ is a continuous function of $\mu$ and $\mathrm{g}(0) = \det(A) < 0$, we have $\mathrm{g}(\mu) = \det((1-\mu)A+\mu B) < 0$ for all $\mu \in [0, 1]$ (recall that $g(1) = \det(B) \neq 0$). Clearly, $\det(Q(\mu)_{1,1}) = (1-\mu)a_{1,1}+\mu b_{1,1} > 0$ for all $\mu \in [0, 1]$, since $A_{1,1} > 0$ and $B_{1,1} > 0$; furthermore, $Q(\mu)_{2,2} = (1 - \mu)A_{2,2} + \mu B_{2,2}$ is positive definite for any $t \in [0, 1]$, since $A_{2,2}$ and $B_{2,2}$ are positive definite. Thus $\det(Q(\mu)_{2,2}) > 0$ for all $\mu \in [0, 1]$. Hence, $X^T Q(\mu)X = 0$ is an ellipse for all $\mu \in [0, 1]$, with its center at $R(\mu) = Q(\mu)^{-1}[0, 0, 1]^T$.

Denote $\mathrm{p}(\mu) \equiv R(\mu)^T AR(\mu)$. Then $\mathrm{p}(\mu)$ is a continuous function of $\mu$ in $[0, 1]$. Clearly, $R(0) \in \mathrm{Int}(\mathcal{A})$, since $R(0)$ is the center of $\mathcal{A}$. We have $R(1) \notin \mathcal{A}$ since $R(1)$ is the center of $\mathcal{B}$ and $\mathrm{Int}(\mathcal{A}) \bigcap \mathrm{Int}(\mathcal{B}) = \emptyset$, which is the hypothesis of the lemma. Hence, $\mathrm{p}(0) = R(0)^T AR(0) < 0$ and $\mathrm{p}(1) = R(1)^T AR(1) > 0$. By continuity argument, it follows that $\mathrm{p}(\mu_1) = 0$ for some $\mu_1 \in [0, 1]$, i.e. the center $R(\mu_1)$ of the ellipse $\mathcal{Q}(\mu_1)$ is on the boundary of the elliptic disk $\mathcal{A}$ (see Fig. 2). Since $\mathcal{A}$ and $\mathcal{B}$ are either separate or touching externally, $\mathrm{Int}(\mathcal{Q}(\mu_1))$ contains a point $X_1$ that is exterior to both $\mathcal{A}$ and $\mathcal{B}$, that

is $X_1^T Q(\mu_1) X_1 < 0$. On the other hand, since $X_1^T A X_1 > 0$, $X_1^T B X_1 > 0$, and $\mu_1 \in (0,1)$, we have

$$X_1^T Q(\mu_1) X_1 = (1-\mu_1) X_1^T A X_1 + \mu_1 X_1^T B X_1 > 0$$

This is a contradiction. Hence, $\mathrm{g}(\mu)$ has a real zero in $(0,1)$. □

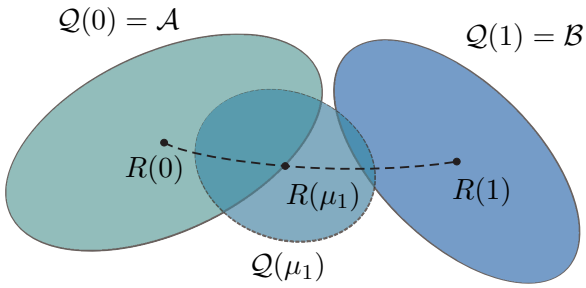


Figure 2: Proof of Lemma 2.

**Lemma 3** *If* $\mathrm{Int}(\mathcal{A}) \bigcap \mathrm{Int}(\mathcal{B}) \neq \emptyset$, *then any real root of* $\mathrm{f}(\lambda) = 0$ *is positive.*

**Proof:** The proof goes by contradiction. Let $\lambda_0$ be a real root of $\mathrm{f}(\lambda) = 0$. Assume $\lambda_0 \leq 0$. Denote $Q_0 = \lambda_0 A - B$. Then there exists a real point $X_0$ such that $Q_0 X_0 = 0$, since $Q_0$ is singular. Since $\mathrm{Int}(\mathcal{A}) \bigcap \mathrm{Int}(\mathcal{B}) \neq \emptyset$, let $X_1 (\neq X_0)$ denote a common interior point of $\mathcal{A}$ and $\mathcal{B}$, i.e., $X_1^T A X_1 < 0$ and $X_1^T B X_1 < 0$ (Fig. 3). Then

$$X_1^T Q_0 X_1 = \lambda_0 X_1^T A X_1 - X_1^T B X_1 > 0.$$

Let $\mathcal{L}$ denote the line passing through $X_0$ and $X_1$. Then, since $\mathcal{A}$ and $\mathcal{B}$ are bounded, there exists on the line $\mathcal{L}$ a point $\tilde{X}$ far enough from $\mathcal{A}$ and $\mathcal{B}$ such that $\tilde{X}$ is exterior to both $\mathcal{A}$ and $\mathcal{B}$. Denote $\tilde{X} = \alpha X_0 + \beta X_1$, where $\alpha$ and $\beta$ are real constants that are not both zero. Then $\tilde{X}^T A \tilde{X} > 0$ and $\tilde{X}^T B \tilde{X} > 0$. It follows that

$$\tilde{X}^T Q_0 \tilde{X} = \lambda_0 \tilde{X}^T A \tilde{X} - \tilde{X}^T B \tilde{X} < 0.$$

On the other hand, since $Q_0 X_0 = 0$ and $X_1^T Q_0 X_1 > 0$, we have

$$\begin{aligned} \tilde{X}^T Q_0 \tilde{X} &= \alpha^2 X_0^T Q_0 X_0 + 2\alpha\beta X_1^T Q_0 X_0 + \beta^2 X_1^T Q_0 X_1 \\ &= \beta^2 X_1^T Q_0 X_1 \geq 0. \end{aligned}$$

This is a contradiction. Hence, any real root $\lambda_0$ of $\mathrm{f}(\lambda) = 0$ is positive. □

**Lemma 4** *If elliptic disks* $\mathcal{A} : X^T A X \leq 0$ *and* $\mathcal{B} : X^T B X \leq 0$ *touch externally, then* $\mathrm{f}(\lambda) = 0$ *has a negative double root.*

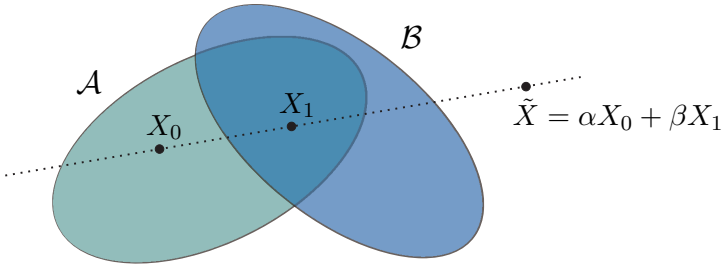


Figure 3: Proof of Lemma 3.

**Proof:** Suppose that $\mathcal{A}$ and $\mathcal{B}$ touch externally. Then the two ellipses $X^T AX = 0$ and $X^T BX = 0$ have a multiple intersection. Then, by [15, page 256], $\mathrm{f}(\lambda) = 0$ has a multiple root $\lambda_0$. Since $\mathrm{Int}(\mathcal{A}) \bigcap \mathrm{Int}(\mathcal{B}) = \emptyset$, by Lemma 2, $\mathrm{f}(\lambda) = 0$ has a negative root $\lambda_1$. Moreover, by Lemma 1, $\mathrm{f}(\lambda) = 0$ has a positive root $\lambda_2$. Thus, we have either $\lambda_0 = \lambda_1 < 0$ or (2) $\lambda_0 = \lambda_2 > 0$. Again, by Lemma 1, only the first case is possible. Hence $\mathrm{f}(\lambda) = 0$ has a negative double root. □

**Lemma 5** *If* $\mathrm{f}(\lambda) = 0$ *has a negative double root, then the elliptic disks* $\mathcal{A} : X^T AX \leq 0$ *and* $\mathcal{B} : X^T BX \leq 0$ *touch each other externally.*

**Proof:** Let $\lambda_0 < 0$ be a negative double root of $\mathrm{f}(\lambda) = 0$. Clearly, $\lambda_0$ is not a zero of the first $2 \times 2$ minors $\det(\lambda A_{2,2} - B_{2,2})$, because both $A_{2,2}$ and $B_{2,2}$ are positive definite and thus the two zeros of $\det(\lambda A_{2,2} - B_{2,2})$ are positive. It follows that $\mathrm{rank}(\lambda_0 A - B) = 2$ and its null space, $\mathrm{Ker}[\lambda_0 A - B]$, has dimension 1.

Since $\det(\lambda A - B) = 0$ has a double root $\lambda_0$, the pencil $X^T(\lambda A - B)X = 0$ contains the singular conic $\lambda_0 A - B$ with multiplicity 2. In this case, the two ellipses $X^T AX = 0$ and $X^T BX = 0$ are tangential to each other at the singular point $X_0$ of the conic $X^T(\lambda_0 A - B)X = 0$, that is, $(\lambda_0 A - B)X_0 = 0$(see [1]).

We are going to show that $X_0$ is a real tangent point of $\mathcal{A}$ and $\mathcal{B}$. Let us suppose that $X_0 = U \pm iV \neq 0$, where $U$ and $V$ are real homogeneous vectors and they are not both zero; without loss of generality, we suppose that $U \neq 0$. Then, from $(\lambda_0 A - B)(U \pm iV) = 0$, it follows that $(\lambda_0 A - B)U = 0$ and $(\lambda_0 A - B)V = 0$. This means that $U$ and $V$ are both real solutions of $(\lambda_0 A - B)X = 0$. Then $U$ and $V$ are linearly dependent, or $V = \alpha U$ from some constant $\alpha$, since $\mathrm{Ker}[\lambda_0 A - B]$ has dimension 1. It follows that $X_0 = (1 + i\alpha)U$ is a real point, since $U$ stands for a real point and the multiplicative constant $(1 + i\alpha)$ can be ignored in homogeneous representation. Hence, the elliptic disks $\mathcal{A}$ and $\mathcal{B}$ touch each other externally at the real point $X_0$. □

The following theorem gives a condition on the separation of two elliptic disks, which is the main result of this section. Fig. 4 illustrates the relationship between two ellipses and the root pattern of their characteristic polynomial.

**Theorem 6** *Given two ellipses* $\mathcal{A} : X^T AX = 0$ *and* $\mathcal{B} : X^T BX = 0$,

1. $\mathcal{A}$ *and* $\mathcal{B}$ *touch externally if and only if* $\mathrm{f}(\lambda) = 0$ *has a negative double root;*

*2. $\mathcal{A}$ and $\mathcal{B}$ are separate if and only if* $\mathrm{f}(\lambda) = 0$ *has two distinct negative roots.*

**Proof:** Part (1) follows from Lemma 4 and Lemma 5. For part (2), the sufficiency follows from Lemma 3 and Lemma 4, and the necessity follows from Lemma 2 and Lemma 5. □

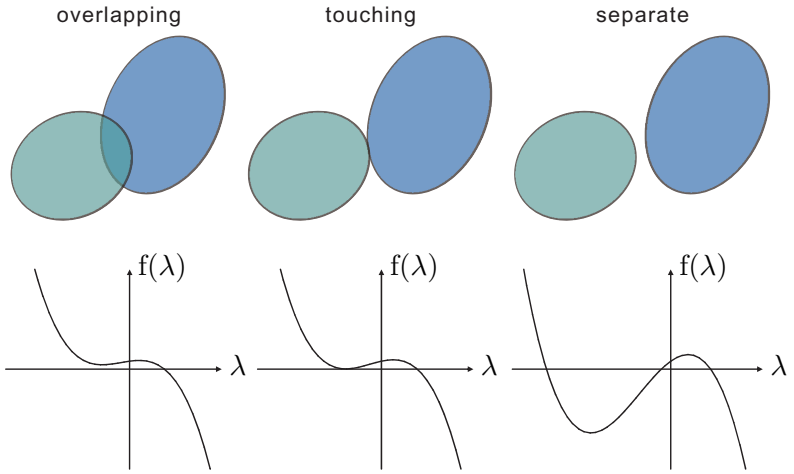


Figure 4: Two elliptic disks and their characteristic polynomial $\mathrm{f}(\lambda)$. Left: Overlapping *if and only if* $\mathrm{f}(\lambda) = 0$ has no negative root. Middle: Touching externally *if and only if* $\mathrm{f}(\lambda) = 0$ has a double negative root. Right: Separate *if and only if* $\mathrm{f}(\lambda) = 0$ has two distinct negative roots.

**Remark**: The application of the above conditions to detecting the overlapping of two stationary ellipses is rather straightforward. A description of the resulting algorithm will be discussed in Section 4 as the first step of our complete algorithm for moving ellipses. Note that the quick and exact overlapping testing of two stationary ellipses should be of interest in its own right in some applications.

The next corollary, following from Theorem 6(2) and Lemma 1, is a key property that enables us to detect collision between two moving elliptic disks $\mathcal{A}(t)$ and $\mathcal{B}(t)$ by the occurrence of a double root of $\mathrm{f}(\lambda; t) = 0$, as will be seen in the next section.

**Corollary 7** *Suppose that two elliptic disks* $\mathcal{A} : X^T AX \leq 0$ *and* $\mathcal{B} : X^T BX \leq 0$ *are separate. Then* $\mathrm{f}(\lambda) = 0$ *does not have any multiple root.*

# 3 Separation Condition for Two Moving Elliptic Disks

In this section we are going to establish a condition for detecting collision of two moving elliptic disks. Consider two elliptic disks $\mathcal{A}(t) : X^T A(t)X \leq 0$ and $\mathcal{B}(t) : X^T B(t)X \leq 0$ in continuous motions $M_A(t)$ and $M_B(t), t \in [0, 1]$ respectively. The disks $\mathcal{A}(t)$ and $\mathcal{B}(t)$ are said to be *collision-free* if $\mathcal{A}(t)$ and $\mathcal{B}(t)$ are separate for all $t \in [0, 1]$; otherwise, $\mathcal{A}(t)$ and $\mathcal{B}(t)$ *collide*, i.e. $\mathcal{A}(t)$ and $\mathcal{B}(t)$ are either touching or overlapping for some $t \in [0, 1]$.

The characteristic polynomial of $\mathcal{A}(t)$ and $\mathcal{B}(t), t \in [0,1]$, is

$$\mathrm{f}(\lambda; t) = \det(\lambda A(t) - B(t)).$$

Write

$$\mathrm{f}(\lambda; t) = \mathrm{g}_3(t)\lambda^3 + \mathrm{g}_2(t)\lambda^2 + \mathrm{g}_1(t)\lambda + \mathrm{g}_0(t). \tag{1}$$

The discriminant of $\mathrm{f}(\lambda; t)$, as a function in $t$, is

$$\Delta(t) = 18\mathrm{g}_3\mathrm{g}_2\mathrm{g}_1\mathrm{g}_0 - 4\mathrm{g}_2^3\mathrm{g}_0 + \mathrm{g}_2^2\mathrm{g}_1^2 - 4\mathrm{g}_3\mathrm{g}_1^3 - 27\mathrm{g}_3^2\mathrm{g}_0^2. \tag{2}$$

(See [7]). By definition, $\mathrm{f}(\lambda; t) = 0$ has a multiple root in $\lambda$ for some $t$ if and only if $\Delta(t) = 0$. Further, it can be shown that $\mathrm{f}(\lambda; t) = 0$ has three simple real roots if $\Delta(t) > 0$ and $\mathrm{f}(\lambda; t) = 0$ has two complex conjugate roots and a real root if $\Delta(t) < 0$.

The next theorem states the condition on two collision-free moving elliptic disks.

**Theorem 8** *Let $\mathcal{A}(t)$ and $\mathcal{B}(t)$, $t \in [0,1]$, be two moving elliptic disks in $\mathbb{E}^2$. Let $\mathrm{f}(\lambda; t)$ be their characteristic polynomial. Let $\Delta(t)$ denote the discriminant of $\mathrm{f}(\lambda; t)$. Suppose that $\mathcal{A}(0)$ and $\mathcal{B}(0)$ are separate. Then $\mathcal{A}(t)$ and $\mathcal{B}(t)$ are collision-free if and only if $\Delta(t)$ has no real zero in $[0,1]$.*

**Proof:** First we prove necessity. Suppose that $\mathcal{A}(t)$ and $\mathcal{B}(t)$ are collision-free. Then by Corollary 7, $\mathrm{f}(\lambda; t) = 0$ does not have a multiple root in $\lambda$ for any $t \in [0,1]$. Therefore, $\Delta(t)$ does not have any real zero in $[0,1]$.

To prove sufficiency, suppose that $\Delta(t) = 0$ has no real root in $[0,1]$. Now assume that $\mathcal{A}(t)$ and $\mathcal{B}(t)$ collide. Then $\mathcal{A}(t_0)$ and $\mathcal{B}(t_0)$ are overlapping or touching for some $t_0 \in [0,1]$. Since $\mathcal{A}(0)$ and $\mathcal{B}(0)$ are separate, by continuity argument, there exists an instant $t_1 \in (0, t_0] \subset [0,1]$ such that $\mathcal{A}(t_1)$ and $\mathcal{B}(t_1)$ touch each other externally. Then, by Theorem 6, $\mathrm{f}(\lambda; t_1) = 0$ has a negative double root in $\lambda$. Therefore $\Delta(t_1) = 0$. But this contradicts that $\Delta(t)$ has no zero in $[0,1]$. Hence, $\mathcal{A}(t)$ and $\mathcal{B}(t)$ are collision-free. □

**Corollary 9** *Let $\mathcal{A}(t)$ and $\mathcal{B}(t)$, $t \in [0,1]$, be two moving elliptic disks. Suppose that $\mathcal{A}(0)$ and $\mathcal{B}(0)$ are separate. If $\Delta(t)$ has a real zero in $[0,1]$, then $\mathcal{A}(t)$ and $\mathcal{B}(t)$ touch each other externally at $t_{\min} \in [0,1]$, where $t_{\min}$ is the smallest real zero of $\Delta(t)$ in $[0,1]$, i.e. $t_{\min} = \min\{t | \Delta(t) = 0, t \in [0,1]\}$.*

The proof of Corollary 9 is similar to the proof of necessity of Theorem 8, so is omitted. Here $t_{\min}$ gives the time of first contact between the disks $\mathcal{A}(t)$ and $\mathcal{B}(t)$.

# 4 Outline of Algorithm

Based on the separation conditions proved in the preceding sections, we shall outline in this section the framework of our algorithm for collision detection of two moving ellipses. Three variants of this algorithm with various enhancements for different types of motions will be discussed in subsequent sections.

**Algorithm:** ***CD-DISC***

**Input:** The matrices $A(t)$ and $B(t)$ of two moving elliptic disks $\mathcal{A}(t)$ and $\mathcal{B}(t)$.

**Output:** Whether the two elliptic disks collide: COLLISION or COLLISION-FREE.

**Step 1:** Compute the characteristic equation $\mathrm{f}(\lambda; 0) = 0$ for $\mathcal{A}(0)$ and $\mathcal{B}(0)$. Then determine whether $\mathrm{f}(\lambda; 0) = 0$ has two distinct negative roots.
If yes, by Theorem 6, $\mathcal{A}(0)$ and $\mathcal{B}(0)$ are separate, and go to Step 2; otherwise, report COLLISION and exit.

**Step 2:** Compute the characteristic polynomial
$$\mathrm{f}(\lambda; t) = \det(\lambda A(t) - B(t)).$$

**Step 3:** Compute the discriminant $\Delta(t)$ of $\mathrm{f}(\lambda; t)$.

**Step 4:** Determine whether $\Delta(t) = 0$ has any real root in $[0, 1]$.
If yes, by Theorem 8, report COLLISION and exit; otherwise, again by Theorem 8, report COLLISION-FREE and exit.

In Step 1 of the algorithm *CD-DISC*, to determine whether or not the two ellipses are separate at $t = 0$, by Theorem 6, we use the Sturm sequence method [7, page 96], a classical real root isolation method, to check whether or not $\mathrm{f}(\lambda; 0) = 0$ has two distinct negative roots. The Sturm sequence method counts the number of real zeros of a polynomial within a specified interval by taking the difference between the numbers of sign changes of the Sturm sequence of the polynomial at two ends of the interval; here a multiple real root is counted once only. When applying the Sturm sequence method to $\mathrm{f}(\lambda; 0)$ on the interval $(-\infty, 0)$, it follows by Lemma 1 that the returned number of zeros can only be 0, 1, or 2, corresponding to that $\mathrm{f}(\lambda; 0) = 0$ has no negative root, one negative double root or two distinct negative roots, respectively.

The algorithm *CD-DISC* reports only whether there is collision between two moving ellipses. By solving for the roots of $\Delta(t)$, this algorithm can be extended to report also the time of first contact or all instants at which two moving ellipses are in external contact. By Corollary 9, the smallest root $t_{\min}$ of $\Delta(t) = 0$ in $[0, 1]$ is always the instant of first contact between the two moving elliptic disks. But, to report all contact instants, the other roots of $\Delta(t) = 0$ in $[0, 1]$ need to be checked for verification, because, while all contact instants must be roots of $\Delta(t) = 0$, a root of $\Delta(t) = 0$ may not correspond to a contact between two elliptic disks; this will be expounded in Section 6.2. Implementation of the algorithm *CD-DISC* with various enhancements for different types of motions and outputs will be discussed in subsequent sections.

# 5 Non-rational Motions

In the algorithm *CD-DISC*, one needs to detect or find the real roots of the univariate equation $\Delta(t) = 0$. When the motion of the ellipses are analytical but otherwise arbitrary,

one needs to solve a rather general equation $\Delta(t) = 0$, which is a general root-finding problem. When the motion is piecewise analytical, the algorithm should be applied for each piece. In the rest of the discussion we shall consider some special types of motions that are frequently encountered and allow relatively easy formulation or efficient handling. Specifically, we will consider the screw motion in this section, and the rational motion in the next section.

The *screw motion* is a simple, commonly used motion. An object assumes a *screw motion* when it is translated with constant velocity and, at the same time, rotates with a constant angular velocity [21]. The entries of the screw motion matrix $M(t)$ contain not only rational functions of time $t$, but also trigonometric terms such as $\cos(\alpha_0 t + \beta_0)$ and $\sin(\alpha_1 t + \beta_1)$ for some constants $\alpha_0, \alpha_1, \beta_0$ and $\beta_1$. Therefore, the coefficients $\mathrm{g}_i(t)$ of the characteristic polynomial in (1) are not rational functions in $t$. Some might suggest that the trigonometric functions be converted into rational functions using the variable substitution $u = \tan(t/2)$. However, this substitution would at the same time make the translational part, which is linear in $t$, non-rational. In fact, the screw motion is intrinsically transcendental; hence, it can only be approximated, but not exactly represented, by a rational motion.

Suppose that two elliptic disks $\mathcal{A}$ and $\mathcal{B}$ move in screw motions. Since the sizes and shapes of the elliptic disks do not change during the motion, the coefficients $\mathrm{g}_3(t)$ and $\mathrm{g}_0(t)$ of (1) are constant and equal to $\det(A)$ and $-\det(B)$, respectively. Let $u = (1-t)\theta_0 + t\theta_1$ and $v = (1-t)\phi_0 + t\phi_1$ be linear interpolations of the end orientation angles $\theta_0$, $\theta_1$ of $\mathcal{A}$ and $\phi_0$, $\phi_1$ of $\mathcal{B}$. Then the other two coefficients $\mathrm{g}_2(t)$ and $\mathrm{g}_1(t)$ can be expressed as

$$\begin{aligned}\mathrm{g}_2(t) = {} & (\alpha_{22}\cos(2v) + \alpha_{21}\sin(2v) + \alpha_{20})t^2 \\ & + (\alpha_{12}\cos(2v) + \alpha_{11}\sin(2v) + \alpha_{10})t \\ & + \alpha_{03}\cos(2(u-v)) + \alpha_{02}\cos(2v) + \alpha_{01}\sin(2v) + \alpha_{00},\end{aligned}$$

and

$$\begin{aligned}\mathrm{g}_1(t) = {} & (\beta_{22}\cos(2u) + \beta_{21}\sin(2u) + \beta_{20})t^2 \\ & + (\beta_{12}\cos(2u) + \beta_{11}\sin(2u) + \beta_{10})t \\ & + \beta_{03}\cos(2(u-v)) + \beta_{02}\cos(2u) + \beta_{01}\sin(2u) + \beta_{00},\end{aligned}$$

where the $\alpha$'s, $\beta$'s are all constants.

Since the coefficients $\mathrm{g}_i(t)$, and hence the discriminant $\Delta(t)$ for a screw motion, are not rational, one may use any numerical solver of choice to compute the roots of $\Delta(t) = 0$ or to check the existence of any real roots. We give en example below to illustrate the steps of the algorithm *CD-DISC* for two ellipses in screw motions.

**Example 1**. Consider two elliptic disks $\mathcal{A} : \frac{x^2}{6^2} + \frac{y^2}{10^2} \leq 1$ and $\mathcal{B} : \frac{x^2}{14^2} + \frac{y^2}{4^2} \leq 1$. Two moving elliptic disks $\mathcal{A}(t)$ and $\mathcal{B}(t)$, $t \in [0, 1]$, are defined by the transformation of $\mathcal{A}$ and $\mathcal{B}$ under

the following screw motions:

$$M_A = \begin{pmatrix} \cos(\frac{10\pi t}{9}) & -\sin(\frac{10\pi t}{9}) & 115t - 80 \\ \sin(\frac{10\pi t}{9}) & \cos(\frac{10\pi t}{9}) & 55t - 38 \\ 0 & 0 & 1 \end{pmatrix}, \quad \text{and}$$

$$M_B = \begin{pmatrix} \cos(\frac{2\pi t}{3}) & -\sin(\frac{2\pi t}{3}) & 76t - 60 \\ \sin(\frac{2\pi t}{3}) & \cos(\frac{2\pi t}{3}) & 97t - 57 \\ 0 & 0 & 1 \end{pmatrix}.$$

The characteristic polynomial is

$$\begin{aligned} \mathrm{f}(\lambda; t) &= \det(\lambda A(t) - B(t)) \\ &= -\tfrac{1}{3600}\lambda^3 + \big((-\tfrac{243}{125440}\cos(\tfrac{4\pi t}{3}) - \tfrac{117}{4480}\sin(\tfrac{4\pi t}{3}) - \tfrac{3869}{125440})t^2 \\ &\quad + (\tfrac{9}{31360}\cos(\tfrac{4\pi t}{2}) + \tfrac{1581}{62720}\sin(\tfrac{4\pi t}{3}) + \tfrac{13939}{470400})t + \tfrac{1}{1960}\cos(\tfrac{8\pi t}{9}) \\ &\quad + \tfrac{39}{125440}\cos(\tfrac{4\pi t}{3}) - \tfrac{19}{3136}\sin(\tfrac{4\pi t}{3}) - \tfrac{10519}{1881600}\big)\lambda^2 \\ &\quad + \big((-\tfrac{27}{39200}\cos(\tfrac{20\pi t}{9}) - \tfrac{13}{1400}\sin(\tfrac{20\pi t}{9}) + \tfrac{1241}{62720})t^2 + (\tfrac{1}{9800}\cos(\tfrac{20\pi t}{9}) \\ &\quad + \tfrac{527}{58800}\sin(\tfrac{20\pi t}{9}) - \tfrac{4471}{235200})t - \tfrac{1}{1960}\cos(\tfrac{8\pi t}{9}) + \tfrac{13}{117600}\cos(\tfrac{20\pi t}{9}) \\ &\quad - \tfrac{19}{8820}\sin(\tfrac{20\pi t}{9}) + \tfrac{937}{313600}\big)\lambda + \tfrac{1}{3136} \end{aligned}$$

The discriminant $\Delta(t)$ has a long expression, so is omitted.

The moving disks $\mathcal{A}(t)$ and $\mathcal{B}(t)$ and the graph of their discriminant are shown in Fig. 5. The color coding shows time progression from red to blue. Using Maple with floating point computations of 12 decimal places precision, the roots are found to be at $t = 0.226, 0.393, 0.600$ and $0.731$. Therefore, the two ellipses collide during the screw motion and the first contact is at time $t = 0.226$. Comparing with the results obtained by Maple integer arithmetics except for the last step of root solving using floating point computations, the accuracy of the roots found above is up to 9 decimal places.

# 6 Rational Motions

Recent studies on rational motions [11, 13, 14, 19], and in particular, on planar rational motions [25], have shown that low degree rational motions are adequate to fulfill the need of motion design and representation in robotics and CAD/CAM. The use of rational motions also allows effective numerical processing using various well-developed techniques for processing polynomials. In this section we shall study in detail the application of our method to collision detection of two elliptic disks in rational motions, and, in particular, rational Euclidean motions. The resulting algorithms are also applicable to affine motions that allow continuous deformation of an ellipse, as often desired in computer animation.

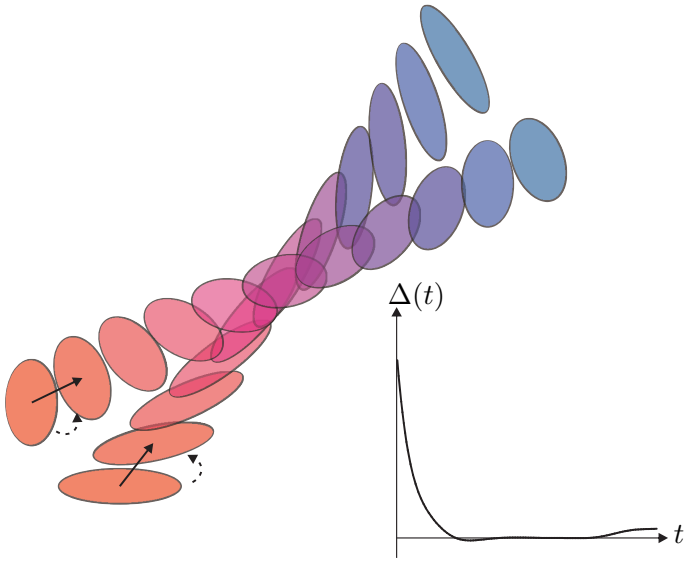


Figure 5: The two moving ellipses in Example 1, progressing from red to blue, and the discriminant $\Delta(t)$.

## 6.1 Planar rational Euclidean motions

We start with a brief review of planar rational Euclidean motions. A Euclidean transformation in $\mathbb{E}^2$ is given by $X' = MX$ where

$$M = \rho \begin{pmatrix} R & V \\ \mathbf{0}^T & 1 \end{pmatrix}$$

for some nonzero constant $\rho$ and $X, X'$ are points in $\mathbb{E}^2$ in homogeneous coordinates. The rotational part of the transformation is described by the $2 \times 2$ orthogonal matrix $R$ and the translational part by the vector $V$. If the entries of $R$ and $V$ are continuous functions of $t$, then $M$ describes a transformation over time and can therefore be denoted by $M(t)$. In particular, if the entries of $M(t)$ are rational functions and $R$ is orthogonal for all $t$, then $M(t)$ is called *a rational Euclidean motion* whose degree is the maximal degree of its entries. (Note that $M(t)$ stands for an affine motion if $R(t)$ is only assumed to be non-singular.)

One way to construct a rational Euclidean motion is to use the kinematic mapping that associates the Euclidean transformation $M$ with a point $\mathbf{d}$ in $\mathbb{P}^3$, the 3D real projective space, as described in [25]. If we write

$$R = \begin{pmatrix} \cos\phi & -\sin\phi \\ \sin\phi & \cos\phi \end{pmatrix} \quad \text{and} \quad V = \begin{pmatrix} v_x \\ v_y \end{pmatrix},$$

then the kinematic image $\mathbf{d} \in \mathbb{P}^3$ of $M$ is given by

$$\mathbf{d} = \begin{pmatrix} d_0 \\ d_1 \\ d_2 \\ d_3 \end{pmatrix} = \begin{pmatrix} v_x \sin(\phi/2) - v_y \cos(\phi/2) \\ v_x \cos(\phi/2) + v_y \sin(\phi/2) \\ -2\cos(\phi/2) \\ 2\sin(\phi/2) \end{pmatrix}.$$

Conversely, any point $\mathbf{d}$ in $\mathbb{P}^3$ with $d_2^2 + d_3^2 \neq 0$ corresponding to a Euclidean transformation $M$ in $\mathbb{E}^2$ is given by

$$M = \begin{pmatrix} d_2^2 - d_3^2 & 2d_2d_3 & 2(d_0d_3 - d_1d_2) \\ -2d_2d_3 & d_2^2 - d_3^2 & 2(d_0d_2 + d_1d_3) \\ 0 & 0 & d_2^2 + d_3^2 \end{pmatrix}. \tag{3}$$

It follows that there is a one-to-one correspondence between a Euclidean transformation in $\mathbb{E}^2$ and a point in the kinematic image space, which is $\mathbb{P}^3$ with the line $d_2 = d_3 = 0$ removed. Due to this correspondence via the kinematic mapping, we may construct a polynomial curve in the kinematic image space and then obtain the corresponding rational Euclidean motion in $\mathbb{E}^2$. In general, if the $d_i$'s are polynomials of degree $n$, the resulting motion will be of degree $2n$. A $C^2$ interpolation scheme of a set of given positions in $\mathbb{E}^2$ with piecewise quartic B-spline rational motions can be found in [25]. Another advantage of rational motions is that they permit an algebraic treatment to the collision detection problem.

When applying a rational motion $M(t)$ to an ellipse $\mathcal{A} : X^T AX = 0$, we get a moving ellipse $\mathcal{A}(t) : X^T A(t)X = 0$ where

$$A(t) = (M^{-1}(t))^T A M^{-1}(t).$$

If $M$ is represented as in (3), then

$$M^{-1} = \begin{pmatrix} d_2^2 - d_3^2 & -2d_2d_3 & 2(d_1d_2 + d_0d_3) \\ 2d_2d_3 & d_2^2 - d_3^2 & 2(d_1d_3 - d_0d_2) \\ 0 & 0 & d_2^2 + d_3^2 \end{pmatrix}.$$

Therefore the maximal degree of the entries in $A(t)$ is $2k$, if the degree of the motion $M(t)$ is $k$.

## 6.2 Properties of $\Delta(t)$

We now analyze the degree of the discriminant $\Delta(t)$. The characteristic equation $\mathrm{f}(\lambda; t) = 0$ of the two moving elliptic disks $\mathcal{A}(t)$ and $\mathcal{B}(t)$ is cubic in $\lambda$, and its degree in $t$ depends on the degree of the rational motions of the two disks. Suppose that the motions $M_A(t)$ and $M_B(t)$ both have degree $k$. Then the maximum degree of the entries in $\lambda A(t) - B(t)$ is $2k$ and the maximum degree of the coefficient $\mathrm{g}_i(t)$ of the characteristic equation is $6k$. Hence, according to (2), the maximum degree of $\Delta(t)$ is $24k$. This analysis gives only an

| Motion Type | Degree in $t$ | | |
|---|---|---|---|
| | $M(t)$ | $\mathrm{g}_i(t)$ | $\Delta(t)$ |
| Linear Translation | 1 | $0_{(\mathrm{g}_0,\mathrm{g}_3)}$, $2_{(\mathrm{g}_1,\mathrm{g}_2)}$ | 8 |
| General Motion | $k$ | $6k$ | $24k$ |

Table 1: Degrees of various entities for rational motions of different degrees. The last row shows the maximum degrees of the entities for a general motion of degree $k$. The motion $M(t)$ takes the form as in Eqn. (3)

upper bound of the degree of $\Delta(t)$, because the actual degree of $\Delta(t)$ depends on particular motions that are used. For example, consider a linear translational motion

$$M(t) = \begin{pmatrix} R(t) & V(t) \\ \mathbf{0}^T & 1 \end{pmatrix},$$

where the entries in $R(t)$ are all constants and those in $V(t)$ are linear polynomials. Then, the degree of $\mathrm{g}_0$ and $\mathrm{g}_3$ is 0 while that of $\mathrm{g}_1$ and $\mathrm{g}_2$ is 2. Therefore the degree of $\Delta(t)$ is only 8, much lower than 24 as deduced from the general analysis. The relationship between the degree of $\Delta(t)$ and the degree of the rational motions is summarized in Table 1.

Now let us consider the geometric meaning of the roots of $\Delta(t)$. If two ellipses $\mathcal{A}(t_0)$ and $\mathcal{B}(t_0)$ touch each other externally, by Theorem 6, $\mathrm{f}(\lambda, t_0) = 0$ has a negative double root, and we have $\Delta(t_0) = 0$. However, when $\Delta(\tilde{t}) = 0$ for some $\tilde{t}$, the disks $\mathcal{A}(\tilde{t})$ and $\mathcal{B}(\tilde{t})$ do not necessarily touch each other.

Fig. 6 shows two elliptic disks moving with linear translational motions and the graph of their discriminant. Here, $\mathcal{A}(0)$ and $\mathcal{B}(0)$ are separate. Note that the first real root $t_1$ of $\Delta(t) = 0$ corresponds to an external contact of $\mathcal{A}(t)$ and $\mathcal{B}(t)$, while the next two roots $t_2$ and $t_3$ of $\Delta(t) = 0$ are caused by internal tangency of the two disks.

Since the degree of $\Delta(t)$ is 8 in the case of a linear translational motion, $\Delta(t) = 0$ can have eight real roots at most. Fig. 7 illustrates a case where all these eight real roots are accounted for by real tangency between two elliptic disks in linear motions. Here, there are two instants ($t_2$ and $t_4$) when the two disks are internally tangential to each other simultaneously at two points; these two instants $t_2$ and $t_4$ are double zeros of $\Delta(t) = 0$.

We have mentioned that a real zero of $\Delta(t) = 0$ may not correspond to any real tangency between the two ellipses. To see this, consider two moving circular disks that become two concentric circles $x^2 + y^2 = 1$ and $x^2 + y^2 = 4$ at time $t_0$. It is easy to verify that the characteristic equation $\mathrm{f}(\lambda; t_0) = 0$ has a positive double root and therefore $\Delta(t_0) = 0$. But the two circles have no *real* touching point; as a matter of fact, the two circles are tangential to each other at two complex conjugate points $(1, \pm i, 0)$, known as the circular points in projective geometry. This explains why only the first real root of $\Delta(t)$ in $t \in [0, 1]$ always indicates an external contact between two moving elliptic disks, as assured by Corollary 9, supposing that the two elliptic disks are separate at the beginning (i.e. when $t = 0$). For each of the other real roots $\bar{t}$ of $\Delta(t) = 0$, we need to check the root pattern of the characteristic polynomial at the time $\bar{t}$ to see whether there is an external contact, using

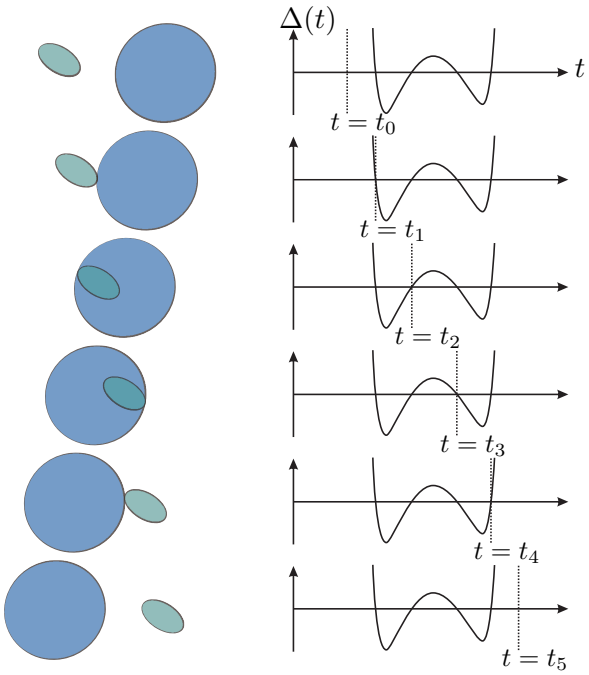


Figure 6: Two elliptic disks with translational motions and their corresponding discriminant function.

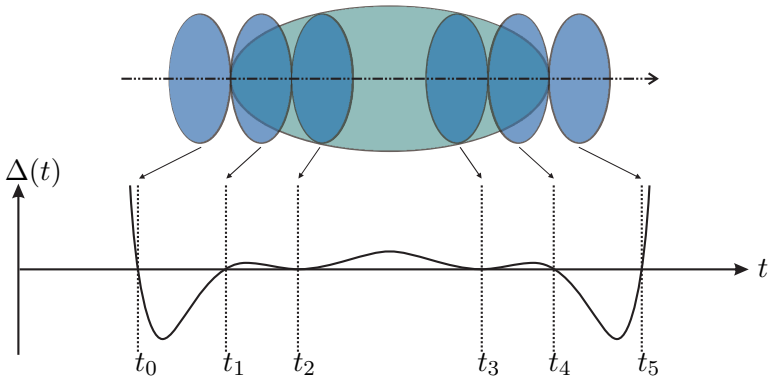


Figure 7: The eight real roots of $\Delta(t) = 0$ for a translational motion and their corresponding contact points between the two elliptic disks. Note the double roots at $t_2$ and $t_4$.

Theorem 6(a) — a root $\bar{t}$ of $\Delta(t) = 0$ corresponds to an external tangency of the two ellipses if and only if the characteristic polynomial $\mathrm{f}(\lambda; \bar{t}) = 0$ has a negative double root in $\lambda$.

## 6.3 Robust computation

In this section, we shall discuss robust implementation of *CD-DISC* for testing collisions between two elliptic disks moving with rational motions. One of the steps in *CD-DISC*

(see Section 4) is to construct the discriminant $\Delta(t)$. The discriminant is a univariate polynomial in $t$ that is the result of long polynomial computations (mainly polynomial multiplications) from the coefficients of the motion matrices, which are also polynomials. When the computations are carried out using the power series representation of the polynomials (i.e. $\mathrm{p}(t) = \sum_{i=0}^{n} a_i t^i, a_i \in \mathbb{R}$), we have found that *CD-DISC* suffered severely from numerical instability when the degree of motion is higher than 2, using double floating point precision. By comparing all intermediate results in the entire process with exact results produced by a Maple implementation of the same algorithm using integer computations, significant errors in the coefficients of $\Delta(t)$ are revealed. We tested an example of two elliptic disks moving with degree 4 motion using high precision floating point computation in Maple, and found that acceptable results could only be obtained when the number of decimal places in the floating point computation is increased to above 20. In this case, the degree of $\Delta(t)$ is 96.

To overcome this numerical instability in processing high degree polynomials, we turned to use the Bernstein form of polynomials. The Bernstein form has the expression $\sum_{i=0}^{n} \binom{n}{i} a_i t^i (1-t)^{n-i}$, $a_i \in \mathbb{R}$, and is known to be numerically more stable for polynomial computations than the power form [9, 20]. In our current implementation of *CD-DISC*, we still use polynomials in the power form when computing the characteristic equation $\mathrm{f}(\lambda; \mathrm{t}) = 0$ from the motion matrices, and then convert the coefficients $\mathrm{g}_i(t)$ of $\mathrm{f}(\lambda; \mathrm{t}) = 0$ into the Bernstein form; the numerical condition of this conversion is still good since the $\mathrm{g}_i(t)$ have relatively low degrees [10]. Finally, we derive $\Delta(t)$ by computing with polynomials in the Bernstein form. Our experiments show that this adoption of the Bernstein form significantly improves the robustness and accuracy of our collision detection procedure.

Now that the discriminant $\Delta(t)$ is obtained in a robust manner, the next step is to analyze its zeros. The level of processing $\Delta(t)$ depends on what kind of collision detection output is required by an application. The following three variants of *CD-DISC* have been implemented that give different collision detection outputs for two elliptic disks moving in rational motions:

**Variant 1:** *reports whether the two elliptic disks collide.*

**Variant 2:** *reports whether the two elliptic disks collide, and if yes, reports the time of first contact.*

**Variant 3:** *reports whether the two elliptic disks collide, and if yes, reports all instants of external contact.*

The above output requirements entail different ways of handling the discriminant $\Delta(t) = 0$. For Variant 1, we only need to check for the existence of real roots of $\Delta(t) = 0$. Here we make use of a recent result that uses an idea similar to the Sturm sequence method to count the number of real roots of a polynomial in the scaled Bernstein form [16], which is expressed as $\sum_{i=0}^{n} b_i t^i (1-t)^{n-i}$, where $b_i \in \mathbb{R}$. This method inherits the robust polynomial computations provided by the Bernstein form and therefore is suitable for high degree polynomials. With this technique, we are able to robustly determine whether $\Delta(t)$ has any real roots in the time interval $t \in [0, 1]$. Here, the coefficients $\mathrm{g}_i(t)$ of the characteristic

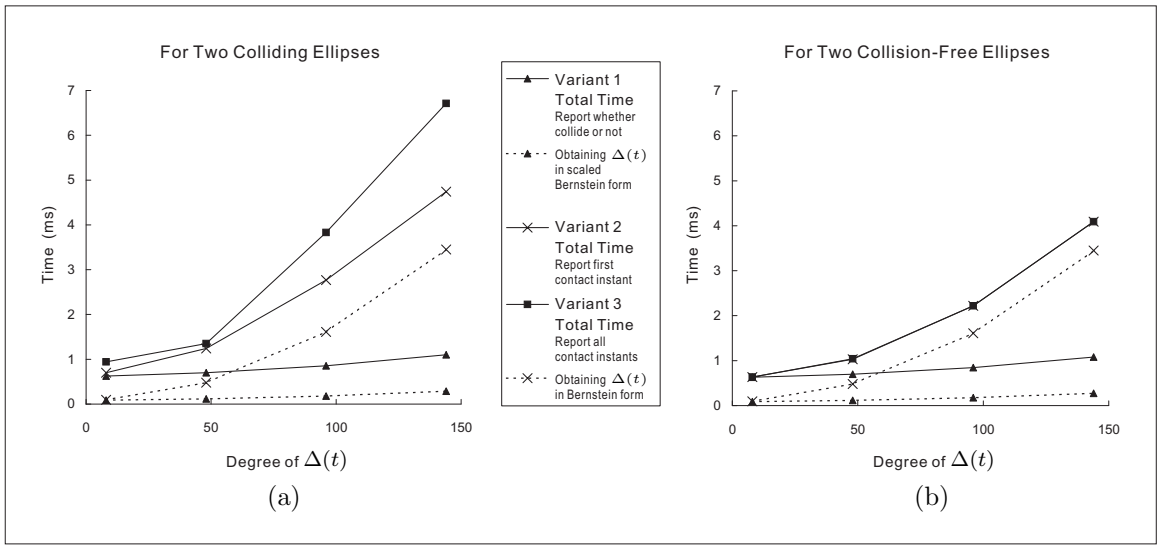


Figure 8: Average CPU time needed for *CD-DISC* to detect collision for two moving elliptic disks with different degrees of motion, when the two moving elliptic disks collide (a) or are collision-free (b). The solid lines show the total collision detection time for the three variants of *CD-DISC* (see text) and the dashed lines show the computation time taken for obtaining $\Delta(t)$ in the Bernstein form and the scaled Bernstein form.

equation $\mathrm{f}(\lambda;\mathrm{t}) = 0$ are first transformed to the scaled Bernstein form and then $\Delta(t)$ is obtained by computing with polynomials in the scaled Bernstein form. This treatments avoids the errors that would otherwise be caused by the high degree of $\Delta(t)$, if $\Delta(t)$ were first obtained in Bernstein basis and then be transformed into the scaled Bernstein form. The scaled Bernstein form is used only in Variant 1.

For Variant 2, we need to solve for the smallest real root of $\Delta(t) = 0$ in $[0, 1]$, if one exists. For Variant 3, in addition to solving for all the real roots of $\Delta(t) = 0$ in $[0, 1]$, for each of these roots we also need to check for the existence of a negative double root of the characteristic polynomial in order to verify the external tangency of the two elliptic disks. In both Variant 2 and Variant 3, we use the de Casteljau algorithm to subdivide $\Delta(t)$ in the Bernstein form to locate all real roots of $\Delta(t)$ in $[0, 1]$. By the convex hull property, we can discard an interval of $t$ if the Bernstein coefficients of $\Delta(t)$ over the interval are all positive or all negative. For Variant 2 where only the first contact time instant is needed, we save time by continuing to subdivide only those intervals that are likely to contain the smallest real root.

## 6.4 Experimental results

We shall first use a designed data set to study the efficiency of our collision detection algorithm, and use an example to show the accuracy of the method. We generated 2,000 test cases for each of the four kinds of motions: linear translation and general degree 2,

degree 4 and degree 6 rational motions. Among each set of 2,000 cases, 1,000 cases were randomly generated pairs of colliding elliptic disks, and the other 1,000 were randomly generated pairs of collision-free elliptic disks. The experiments were run on a PC with a 2.2GHz Intel CPU and the timing results are shown in Fig. 8. The graphs in Fig. 8(a) and Fig. 8(b) give the average CPU time taken to detect collisions by *CD-DISC* for colliding and collision-free elliptic disks, respectively. The three solid lines correspond to the three different outputs (Variants 1, 2 & 3 as in Section 6.3) that *CD-DISC* can report. Clearly, more time is needed as the degree of motion and hence the degree of $\Delta(t)$ increases. For two elliptic disks with degree 6 motion, for which the degree of $\Delta(t)$ is 144, it takes less than 1 ms to determine whether there is collision, less than 5 ms to compute the instant of first contact, and less than 7 ms to compute all instants of contact.

For both colliding and collision-free ellipses, the algorithm takes the same time for Variant 1 where it is only required to detect whether there is collision, since the computation involved (i.e. to determine root existence by Sturm sequences) in both colliding and collision-free cases are the same. In the case for colliding elliptic disks (Fig. 8a), more time is needed for Variant 2 and Variant 3 to detect the instants of contacts; in general, the computation time increases as the number of roots) of $\Delta(t)$ increases. For collision-free ellipses (Fig. 8b), since $\Delta(t)$ has no root, the average CPU time taken for reporting the instant of first contact (Variant 2) or the instants of all contacts (Variant 3) are the same.

The dashed lines in the graphs show the time needed for obtaining the polynomial $\Delta(t)$ from the characteristic equation; in Variant 1, $\Delta(t)$ is obtained in the scaled Bernstein form while in Variant 2 and Variant 3, the computation is done in the Bernstein form. It is obvious that in Variant 2 and Variant 3, the time for getting $\Delta(t)$ constitutes the major portion of the overall time for collision detection. Polynomial multiplications in the scaled Bernstein form are much more efficient than that in the Bernstein form, explaining why the time needed for obtaining $\Delta(t)$ in Variant 1 is much less than that needed in Variant 2 and Variant 3.

Next, we use an example to show the robustness of the algorithm *CD-DISC*.

**Example 2**. Consider two ellipses $\mathcal{A} : \frac{x^2}{5^2} + \frac{y^2}{10^2} = 1$ and $\mathcal{B} : \frac{x^2}{5^2} + \frac{y^2}{10^2} = 1$. Two moving elliptic disks $\mathcal{A}(t)$ and $\mathcal{B}(t)$, $t \in [0, 1]$, are defined by applying to $\mathcal{A}$ and $\mathcal{B}$ the following motions $M_A$ and $M_B$:

$$M_A = \begin{pmatrix} -16t^4 + 32t^3 - 16t + 4 & -32t^3 + 48t^2 - 16t & -160t^3 - 240t^2 + 160t - 40 \\ 32t^3 - 48t^2 + 16t & -16t^4 + 32t^3 - 16t + 4 & 480t^4 - 960t^3 + 880t^2 - 400t + 80 \\ 0 & 0 & 16t^4 - 32t^3 + 32t^2 - 16t + 4 \end{pmatrix},$$

$$M_B = \begin{pmatrix} -16t^4 + 32t^3 - 16t + 4 & 32t^3 - 48t^2 + 16t & 160t^3 - 240t^2 + 160t - 40 \\ -32t^3 + 48t^2 - 16t & -16t^4 + 32t^3 - 16t + 4 & -480t^4 + 960t^3 - 880t^2 + 400t - 80 \\ 0 & 0 & 16t^4 - 32t^3 + 32t^2 - 16t + 4 \end{pmatrix}.$$

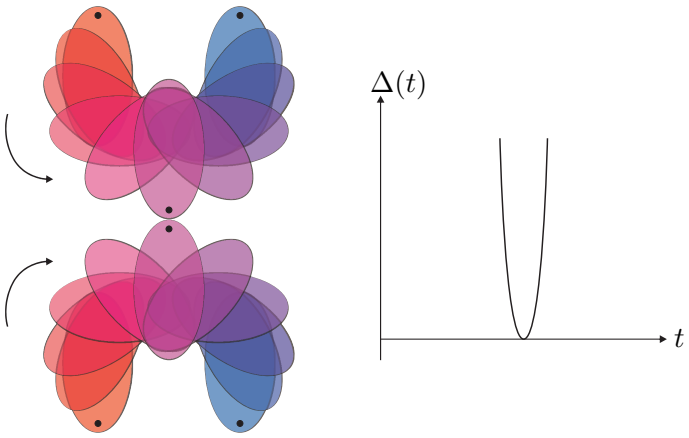


Figure 9: The two moving elliptic disks in Example 2 and their discriminant $\Delta(t)$.

The characteristic equation is

$$
\begin{aligned}
&\mathrm{f}(\lambda;t) = \det(\lambda A(t) - B(t)) \\
&= (-4096t^{24} + 49152t^{23} - 294912t^{22} + 1171456t^{21} - 3446784t^{20} + 7974912t^{19} \\
&\quad - 15048704t^{18} + 23721984t^{17} - 31756032t^{16} + 36517888t^{15} - 36360192t^{14} \\
&\quad + 31509504t^{13} - 23835904t^{12} + 15754752t^{11} - 9090048t^{10} + 4564736t^{9} - 1984752t^{8} \\
&\quad + 741312t^{7} - 235136t^{6} + 62304t^{5} - 13464t^{4} + 2288t^{3} - 288t^{2} + 24t - 1)\lambda^{3} \\
&\quad + (-135168t^{24} + 1622016t^{23} - 11304960t^{22} + 55959552t^{21} - 206878720t^{20} \\
&\quad + 588967936t^{19} - 1325514752t^{18} + 2409461760t^{17} - 3596409600t^{16} + 4461631488t^{15} \\
&\quad - 4639457280t^{14} + 4065807360t^{13} - 3011391744t^{12} + 1886084608t^{11} - 997282816t^{10} \\
&\quad + 443501312t^{9} - 164884848t^{8} + 50819520t^{7} - 12842880t^{6} + 2624352t^{5} - 426168t^{4} \\
&\quad + 53808t^{3} - 5120t^{2} + 344t - 13)\lambda^{2} \\
&\quad + (135168t^{24} - 1622016t^{23} + 11304960t^{22} - 55959552t^{21} + 206878720t^{20} \\
&\quad - 588967936t^{19} + 1325514752t^{18} - 2409461760t^{17} + 3596409600t^{16} - 4461631488t^{15} \\
&\quad + 4639457280t^{14} - 4065807360t^{13} + 3011391744t^{12} - 1886084608t^{11} + 997282816t^{10} \\
&\quad - 443501312t^{9} + 164884848t^{8} - 50819520t^{7} + 12842880t^{6} - 2624352t^{5} + 426168t^{4} \\
&\quad - 53808t^{3} + 5120t^{2} - 344t + 13)\lambda \\
&\quad + 4096t^{24} - 49152t^{23} + 294912t^{22} - 1171456t^{21} + 3446784t^{20} - 7974912t^{19} \\
&\quad + 15048704t^{18} - 23721984t^{17} + 31756032t^{16} - 36517888t^{15} + 36360192t^{14} \\
&\quad - 31509504t^{13} + 23835904t^{12} - 15754752t^{11} + 9090048t^{10} - 4564736t^{9} + 1984752t^{8} \\
&\quad - 741312t^{7} + 235136t^{6} - 62304t^{5} + 13464t^{4} - 2288t^{3} + 288t^{2} - 24t + 1 \\
&= 0,
\end{aligned}
$$

and the discriminant $\Delta(t)$ is of degree 96 and is omitted here. Fig. 9 shows the two moving elliptic disks and the graph of $\Delta(t)$. The two disks are designed to only touch each other externally at $t = 0.5$ and are separate for the rest of the time. In our experiments all the three variants of *CD-DISC* determined correctly that there is a contact and Variant 2 and Variant 3 reported accurately the contact time at $t = 0.5$. To examine the sensitivity

of *CD-DISC*, the lower disk in Fig. 9 is translated by a little amount in the negative $y$ direction so that the two moving disks attain a minimum separating distance $d > 0$ at $t = 0.5$. It has been found that, for this setup, *CD-DISC* reports collision when $d < 10^{-6}$, and reports non-collision for larger values of $d$. We believe that this precision is adequate for most practical applications in robotics.

# 7 Conclusion

We have presented a collision detection algorithm for two elliptic disks moving with continuous motions in the 2D plane. The algorithm, called *CD-DISC*, is based on an algebraic characterization of two collision-free elliptic disks, which can assume rigid or deformable motions. *CD-DISC* uses exact representations for ellipses and therefore does not suffer from errors induced by polygonal approximations. This algorithm determines collision by checking for the existence of real roots of a univariate function which is the discriminant of the characteristic equation of the two moving ellipses. Unlike many other collision detection algorithms, *CD-DISC* does not use temporal sampling on the motion path so that inaccuracy due to limited sampling resolution is avoided.

We have studied in detail the commonly used screw motions and rational motions. For motions that are intrinsically non-rational, such as the screw motion, the algorithm can be used with the aid of a numerical solver of a univariate function. Rational motions are considered because they are flexible enough for modeling general motions and their polynomial representation makes an algebraic treatment to collision detection possible; in fact, in this case the collision detection is achieved by detecting or finding the real roots of a univariate polynomial. We have demonstrated that the use of Bernstein forms for polynomial manipulation significantly increases numerical stability of *CD-DISC* for high degree rational motions, in conformation with the observations made in [9, 10, 20]. Our experiments show that *CD-DISC* is fast and accurate for detecting collisions between moving ellipses under continuous rational motions of degree six or less; note that research [25] in planar rational motions suggests that rational motions of degree four are already adequate for modeling smooth motions in practice.

There are several problems open for further research. The minimum distance of two collision-free moving elliptic disks can be useful for motion path planning. Therefore further work is needed to study the relationship between the minimum distance between two separate elliptic disks and the value of the discriminant $\Delta(t)$. An observation is that the difference between the two negative roots of the characteristic polynomial becomes smaller as the two separate disks approach each other gradually and eventually the two roots merge into a negative double root when the two disks become externally tangential to each other, signaled by the vanishing of the discriminant function.

Devising an algebraic approach to continuous collision detection of moving ellipsoids in 3D space is another interesting but challenging problem. Unfortunately, it is not a straightforward task to extend the algorithm *CD-DISC* directly to moving ellipsoids in 3D. It is proved in [26] that the quartic characteristic equation $\mathrm{f}(\lambda) \equiv \det(\lambda \mathrm{A} - \mathrm{B}) = 0$ of

two ellipsoids in 3D space always has two positive roots, and two ellipsoids are separate if and only if $f(\lambda) = 0$ has two distinct negative roots. Unlike the case of elliptic disks (ref. Corollary 7), the characteristic equation $f(\lambda) = 0$ may have a positive double root for a pair of separate ellipsoids; one may check the characteristic equation of two separate spheres, which always has a double root $\lambda = 1$. Thus if we rely on detecting real zeros of the discriminant for collision detection of moving ellipsoids, the algorithm will certainly fail, i.e. have a false positive, because a zero of the discriminant can be caused by a positive double root, which does not correspond to an external contact between the two ellipsoids. To circumvent the above difficulty, a method is proposed in [5] for continuous collision detection of ellipsoids by analyzing the zero-set topology of the bivariate function $f(\lambda; t) = 0$. The main issue with this method is how to efficiently extract and parse the topology of the zero set of a high degree bivariate polynomial resulting from general rational motions.

# References


[1] M. Berger, *Geometry, Vol. II*. Berlin: Springer-Verlag, 1987.

[2] T. J. IÁ. Bromwich, *Quadratic Forms and Their Classification by Means of Invariant-Factors*. New York: Hafner Publishing Co., 1906.

[3] R. Bhatia, *Matrix Analysis, Graduate Textbook of Mathematics, Vol. 169*. New York: Springer, 1997.

[4] S. Cameron, "Collision Detection by Four-Dimensional Intersection Testing," *IEEE Trans. Robot. Automat.*, vol. 6, no. 3, pp. 291–302, 1990.

[5] Y. K. Choi, W. Wang and M.-S. Kim, "Exact Collision Detection of Two Moving Ellipsoids under Rational Motions," in *Proc. IEEE Int. Conf. Robotics and Automation*, 2003, pp. 349–354.

[6] A. P. Del Pobil and M. A. Serna, *Spatial Representation and Motion Planning*. Springer, 1995.

[7] L. Dickson, *Elementary Theory of Equations*. New York: Wiley, 1914.

[8] G. Elber and M.-S. Kim, "Geometric constraint solver using multivariate rational spline functions," in *Proc. of the 6th ACM Symposium on Solid Modeling and Applications*, Ann Arbor, Michigan, USA, June 4–8, 2001, pp. 1–10.

[9] R. T. Farouki and V. T. Rajan, "On the numerical condition of polynomials in Bernstein form," *Comput. Aided Geom. D.*, vol. 4, pp. 191–216, 1987.

[10] R. T. Farouki, "On the stability of transformations between power and Bernstein polynomial forms," *Comput. Aided Geom. D.*, vol. 8, pp. 29–36, 1991.

[11] T. Horsch and B. Jüttler, "Cartesian spline interpolation for industrial robots," *Comput. Aided Design*, vol. 30, no. 3, pp. 217–224, 1998.

[12] P. Jiménez, F. Thomas, and C. Torras, "3D Collision Detection: A Survey," *Comput. Graph.*, vol. 25, no. 2, pp. 269–285, 2001.

[13] B. Jüttler and M. G. Wagner, "Computer-aided design with spatial rational B-spline motions," *ASME Journal of Mech. Design*, vol. 116, 1996, pp. 193–201.

[14] B. Jüttler and M. G. Wagner, "Kinematics and Animation," in G. Farin, J. Hoschek, and M.-S. Kim, editors, *Handbook of Computer Aided Geometric Design*. North-Holland, 2002, pp. 723–748.

[15] H. Levy, *Projective and Related Geometries*. New York: Macmillan, 1964.

[16] H. M. Möller, "Counting zeros of polynomials by their Bézier ordinates," *Ergebnisbericht*, Nr. 251, Universität Dortmund, 2004.

[17] C. Ó Dúnlaing and C. K. Yap, "A Retraction Method for Planning the Motion of a Disc," *J. Algorithm.*, vol. 6, pp. 104–111, 1985.

[18] F. P. Preparata and M. I. Shamos, *Computational Geometry: An Introduction*. New York: Springer-Verlag, 1985.

[19] O. Röschel, "Rational motion design – a survey," *Comput. Aided Design*, vol. 30, no. 3, pp. 169–178, 1998.

[20] T. W. Sederberg, "Applications to computer aided geometric design," in *Proc. of Symposia in Applied Mathematics*, **53**, American Mathematical Society, 1998, pp. 67–89.

[21] J. M. Selig, *Geometric Methods in Robotics*. New York: Springer-Verlag, 1996.

[22] J. T. Scwhartz, M. Sharir and J. Hopcroft, *Planning, Geometry, and Complexity of Robot Motion*. Ablex Publishing Corporation, 1987.

[23] M. I. Shamos and D. Hoey, "Geometric intersection problems," in *Proc. 17th Annu. IEEE Sympos. Found. Comput. Sci.*, 1976, pp. 208– 215.

[24] M. Sharir, "Intersection and closest-pair problems for a set of planar discs," *SIAM J. Comput.*, vol. 14, no. 2, pp. 448–468, May 1985.

[25] M. G. Wagner, "Planar Rational B-Spline Motions," *Comput. Aided Design*, vol. 27, no. 2, pp. 129–137, 1995.

[26] W. Wang, J. Wang, and M.-S. Kim, "An algebraic condition for the separation of two ellipsoids," *Comput. Aided Geom. D.*, vol. 18, pp. 531–539, 2001.